Article

A Single Biosensor for Simultaneous Quantification of Glucose and pH in a Rat Brain of Diabetic Model using Both Current and Potential Outputs

Shuai Li, Anwei Zhu, Tong Zhu, John ZH. Zhang, and Yang Tian

Anal. Chem., **Just Accepted Manuscript** • Publication Date (Web): 31 May 2017

A Single Biosensor for Simultaneous Quantification of Glucose and pH in a Rat Brain of Diabetic Model using Both Current and Potential Outputs

Shuai Li, Anwei Zhu,* Tong Zhu, John ZH. Zhang, Yang Tian*

Shanghai Key Laboratory of Green Chemistry and Chemical Processes, School of Chemistry and Molecular Engineering, East China Normal University, Dongchuan Road 500, Shanghai 200241, P.R. China

ABSTRACT: Glucose and pH are two important indicators of diabetes mellitus. However, their dynamic changes at the same time in brain are still not clear, mainly due to a lack of a single biosensor capable of simultaneous quantification of two species in a live rat brain. In this work, a selective and sensitive ratiometric electrochemical biosensor was developed for simultaneously quantifying glucose and pH using both current and potential outputs in a rat brain of diabetic model. Here, glucose oxidase was first employed as a specific recognition element for both glucose and pH because the active center (FAD) could undergo a $2H^+/2e^-$ process. Moreover, an insensitive molecule toward pH and glucose was used as an inner-reference element to provide a built-in correction to improve the accuracy. The ratio between the oxidation peak current density of glucose and that of ABTS gradually increased with increasing concentration of glucose, and showed a good linearity in the range of 0.3-8.2 mM. Meanwhile, the mid-potential difference between glucose oxidase and 2, 2'-azino-bis (3-ethylbenzthiazoline-6-sulfonic acid) (ABTS) positively shifted with pH decreasing, leading to accurate determination of pH in the linear range of 5.67-7.65. Thus, combined with the unique properties of carbon fiber microelectrode including easy to insert and good biocompatibility, the developed single biosensor was successfully applied to detect pH and glucose at the same time in hippocampus, striatum, and cortex in a live rat brain of diabetic model.

Since glucose provides almost exclusive metabolic energy for brain and may activate neurons in the peripheral and central nervous systems, dysfunction of glucose metabolism can trigger wide spread disease of the peripheral and central nervous systems as well as cardiovascular disease, nephropathy, retinopathy.[1-3] Indeed, decreased glucose metabolism usually precede the emergence of brain pathology and cognitive impairment.[4,5] On the other hand, under a condition of diabetes mellitus, mitochondria, mainly responsible for the synthesis of ATP required for neural cell function, has also been found to produce much larger amounts of H^+. This large amount of H^+ is released via various types of ion transporters to the extra-cellular space, resulting in lowered pH of the interstitial fluid.[6,7] Note that even a slight change in pH can cause severe effects on the biochemical, ion-regulatory, or electrical machinery of nerve and glial cells. Brain acidosis will augment cell death under various pathological conditions.[8,9] Although both glucose and pH are involved in diabetes mellitus, attempts so far to simultaneous in vivo monitoring of pH and glucose for exploring their relationship still have not been reported. Therefore, new tactics toward in vivo analysis of pH and glucose in diabetic rat brain are highly desired and crucial to the field.

Up to now, several efficient approaches for determination of glucose or pH alone have been developed, including fluorescence sensing,[9-13] electrochemical assays,[14-18] and colorimetric.[19] Among these approaches, electrochemical technique shows obvious advantages in sensitivity and simplicity, particularly for real-time measurements and in vivo analysis.[20-22] We have recently developed a single biosensor for monitoring two species (Cu^{2+} and L-Cysteine) in live rat brain based on an electrochemical signal switching on and off.[23,24] However, the strategy could not simultaneously detect two molecules in vivo. Kim have reported a skin-mounted graphene-hybrid device arrays to simultaneous monitor glucose and pH in sweat.[25] But two independent functional units (glucose oxidase and polyaniline) were required to sense glucose and pH respectively by different analytical principles and the biosensor was unavailable for in vivo determination in brain.

Herein, a single ratiometric biosensor with high accuracy, sensitivity and selectivity was first developed for simultaneously quantifying the levels of pH and glucose using both current and potential outputs in a live rat brain of diabetic model. Glucose oxidases (GOD) have been widely used in the design of glucose biosensor due to their specificity to glucose.[26,27] The electrochemical response of GOD on electrodes originated from the redox reaction of FAD encapsulated in the enzyme molecule. Meanwhile, FAD is known to undergo a two-electron coupled with two-proton redox reaction. As shown in Scheme 1, GOD was first employed as a specific recognition element for both pH and glucose, through current and potential outputs. Meanwhile, an insensitive molecule toward pH and glucose, 2, 2′-azino-bis (3-ethylbenzthiazoline-6-sulfonic acid) (ABTS) served as reference signal for providing built-in correction to avoid brain environmental effect. In addition, a stable platform consisting of single-walled carbon nanotube (SWNT) assembled on carbon fiber microelectrode (CFME) greatly improved the direct electron transfer of GOD for quantification of pH and

glucose.[28-30] Accordingly, a single ratiometric biosensor was developed for simultaneous determination of pH and glucose with high selectivity, accuracy, and sensitivity. On one hand, the ratio between the oxidation peak current density of glucose and that of ABTS gradually increased with increasing concentration of glucose, and showed a good linearity in the range of 0.3-8.2 mM. On the other hand, the mid-potential difference between glucose oxidase and t ABTS positively shifted with pH decreasing, leading to accurate determination of pH in the linear range of 5.67-7.65, which fulfills the requirements for in vivo detection in the biological system. Finally, combined with unique properties of CFME including easy to insert and good biocompatibility in the live brain,[18,31,32] the developed single biosensor was successfully applied in directly evaluating the levels of pH and glucose in a live rat brain of diabetic model.

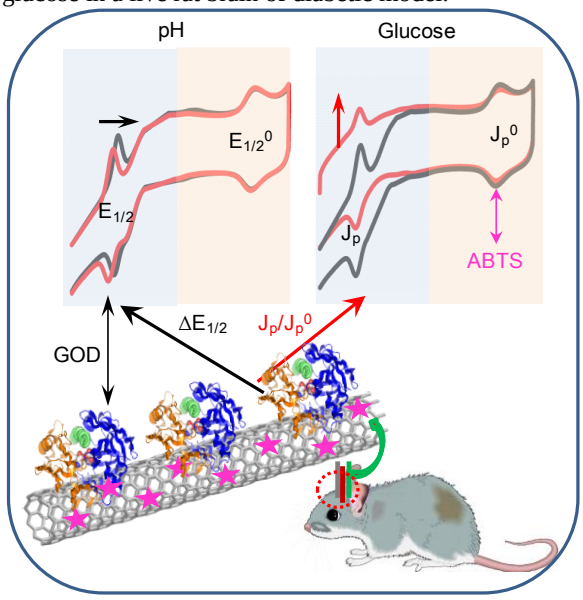

Scheme 1. The developed ratiometric electrochemical biosensor for simultaneous detection and real-time quantification of pH and glucose sensor in a rat brain.

EXPERIMENTAL SECTION

Reagent and Chemicals. Glucose oxidase (GOD, EC 1.1.3.4, type X-S, 100-250 units/mg, from Aspergillus niger), β-D(+)-glucose, 2, 2'-Azinobis-(3-ethylbenzthiazoline-6-sulphonate) (ABTS), Phosphate Buffered Saline (PBS, 10 mM), glutaraldehyde (GA, 50%), uric acid (UA), ascorbic acid (AA), dopamine (DA), DOPAC, 30% hydrogen peroxide (H_2O_2) $NaNO_2$, and NaClO were purchased from Sigma-Aldrich. L-arginine (Arg), L-cysteine (Cys), L-lysine (Lys), L-histidine (His), L-glutamine (Glu), L-isoleucine (Iso), L-leucine (Leu), glycine (Gly), L-threonine (Thr), L-valine (Val), L-methionine (Met), L-serine (Ser), L-phenylalanine (Phe), 5-hydroxyindole-3-acetic acid (5-HIAA), 3-methoxytyramine hydrochloride (3-MT), adenosine 5'-triphosphate disodium salt hydrate (ATP), homovanillic acid (HVA), L-tyrosine, DL-lactic acid and tyramine were purchased from Sigma Aldrich. Metal chloride salts including NaCl, KCl, $CaCl_2$, $AlCl_3$, $ZnCl_2$, $PbCl_2$, $MgCl_2{\cdot}6H_2O$, $CuCl_2{\cdot}2H_2O$, $BaCl_2{\cdot}2H_2O$, $FeCl_3{\cdot}6H_2O$, $FeCl_2{\cdot}4H_2O$, $CoCl_2{\cdot}6H_2O$, $CdCl_2{\cdot}2.5H_2O$, $NiCl_2{\cdot}6H_2O$, and $CrCl_3{\cdot}6H_2O$ were purchased from Aladdin Chemistry Co. Ltd. (Shanghai, China). Single-walled carbon nanotube (SWNT) were purchased from Nanoport Co. Ltd. (Shenzhen, China). Prior to use, SWNT were purified by refluxing the as-received SWNT in 2.6 M nitric acid for 5 h followed by centrifugation, resuspension, filtration, and air-drying to evaporate the solvent. Artificial cerebrospinal fluid (aCSF) was prepared by mixing NaCl (126 mM), KCl (2.4 mM), KH_2PO_4 (0.5 mM), $MgCl_2$ (0.85 mM), $NaHCO_3$ (27.5 mM), Na_2SO_4 (0.5 mM), and $CaCl_2$ (1.1 mM) into MilliQ water. The solution pH was adjusted to 7.4 using HCl and NaOH solution under regulation of pH meter. All chemicals were of analytical grade and commercially available. All aqueous solutions were prepared with Milli-Q water (18.2 M Ω cm, Millipore).

In the selectivity test, superoxide anion ($O_2^{\cdot-}$) was generated by dissolving 10 μM KO_2 in the DMSO solution. Hydroxyl radical ($^{\cdot}OH$) was produced by the Fenton reaction (H_2O_2: Fe^{2+} = 6:1). Singlet oxygen ($^1O_2$) was generated by H_2O_2 (10 μM) reacted with NaClO (10 μM). Alkyl peroxyl radical ($ROO^{\cdot}$) was chemically generated by thermolysis of 10 μM AAPH in air-saturated solution at 310 K. Hypochlorite anion (ClO^-) was supplied by NaClO (10 μM). Peroxynitrite ($ONOO^-$) was produced by mixing 10 μM $NaNO_2$ and 10 μM H_2O_2.

Preparation and Modification of Electrodes. Carbon fiber microelectrode (CFME) was prepared as below. Briefly, a glass capillary (i.d. 1.2 mm, length 100 mm) was pulled into two conical capillaries with 10-30 μm orifice diameter. A single carbon fiber (8 μm in diameter, Tokai, Japan) was adhered to a bare copper wire by silver conducting adhesive and vacuum dried. Then, the carbon fiber was carefully inserted into the capillary. Both ends of the capillary were sealed with 1:1 (v:v) of ethylenediamine and epoxy resin, and the excessed epoxy on the exposed fiber was removed with acetone. After that, CFME was dried at 120ºC for 2 hours and the exposed carbon fiber was cut to ~500 μm in length under a microscopy. Prior to modification, CFME was sonicated in acetone, 3.0 M HNO_3, 1.0 M KOH, and ultrapure water sequentially to remove the impurities on the surface of electrode. Then, CFME was electrochemical activated in 0.5 M H_2SO_4 as follows, first with amperometry method at +2.0 V for 30 s, -1.0 V for 10 s, and then with cyclic voltammetry within a potential range from 0 V to 1.0 V at a scan rate of 0.1 V s^{-1} until the cyclic voltammogram was stable.

For functional modification, CFME was first modified with SWNT according to a reported method[33,34]. In order to enhance the dispersibility of carbon nanotubes, the single-walled carbon nanotube (SWNT) were oxidized and shortened with 2.6 M nitric acid for 5 h. The acidification treated SWNT can disperse in aqueous solution uniformly. In briefly, one drop of a homogeneous dispersion of SWNT (1 mg mL^{-1}) was dripped onto a smooth glassy plate, and then electrodes were carefully immersed and rolled in the droplet for about 1 min under a microscope. Close attention should be paid not to break carbon fibers during this process. The SWNT-modified electrode was air dried, and then thoroughly rinsed with ultrapure water to remove any loosely adsorbed SWNT on the surface before

further modification. The SWNT-modified CFME was denoted as SWNT/CFME. Then, the SWNT/CFME was immersed into 5 mM ABTS aqueous solution for about 10 min and rinsed with ultrapure water and dried by nitrogen. The obtained electrode was defined as ABTS/SWNT/CFME. Finally, ABTS/SWNT/CFME was immersed into 10 mM PBS containing 5 mM GOD and 1% GA and BSA for 4 h, rinsed with ultrapure water and dried by nitrogen, and the electrode was defined as GOD/ABTS/SWNT/CFME.

Apparatus and Measurements. X-ray photoelectron spectroscopy (XPS) investigation was conducted with PHI-5000C ESCA system (Perkin Elmer) with Mg Ka radiation. SEM images were taken using Hitachi S-4800 scanning electron microscope (Hitachi, Tokyo, Japan). Fourier transform infrared spectroscopy (FTIR, Nicolet iS10, Thermo Electron, America) was used to characterize modification of ABTS and GOD. Electrochemical measurements were carried out using Electrochemical station CHI660A (CH Instruments Shanghai, China) with a three-electrode system, in which CFME was employed as a working electrode, Pt wire as a counter electrode and Ag/AgCl electrode as a reference electrode. All measurements were performed at ambient temperature.

In Vivo Detection. All animal experiments were conducted with approval of the Animal Ethics Committee in East China Normal University, China. Streptozocin (STZ) induced diabetic rats (200 - 300 g adult male Wistar rat) were purchased from Shanghai SLAC Laboratory Animal Co. Ltd. Rats' surgeries were performed as follows. The rats were anesthetized utilizing chloral hydrate (predose of 330 mg/kg). The rats were placed on a heating pad to hold the body temperature and fixed in a stereotaxic frame (Beijing Tide-Gene Biotechnology Development Center). The GOD/ABTS/SWNT /CFME electrode was implanted in the left striatum (AP = 2.0 mm, L = 2.5 mm anterior to bregma, and V = 6.0 mm below dura), the cortex (AP = 0.2 mm, L = 5.6 mm from bregma, V = 2.0 mm below dura), the dorsal hippocampus (AP = 5.0 mm, L = 5.0 mm from bregma, V = 1.5 mm below dura), according to standard stereotaxic procedures. Reference and counter electrodes were introduced through a 2 mm plastical cannula positioned into the dura of the brain. In the process of operation, extra chloral hydrate (100 mg/kg) were injected as required and the body temperature of the animals was maintained at 37°C.

RESULTS AND DISCUSSION

Figure 1A shows typical SEM image of CFME modified with SWNTs (SWNT/CFME). It is clear that SWNTs were assembled on CFME surface with diameter of ~20 nm. Then, the inner reference element – ABTS and responsive element – GOD were immobilized onto SWNT/CFME electrode, as illustrated in Scheme 1. The modification processes were traced by XPS (Figure 1B and 1C) and FTIR spectra (Figure 1D). The observation of S_{2p} (162.5 eV, 167.5 eV) and N_{1s} (398.3 eV, 400.5 eV, 402.5 eV) in Figure 1B and 1C (cure b) demonstrates the successful modification of ABTS on SWNT/CFME surface. S_{2p} peaks located at 162.5 eV and 167.5 eV were ascribed to sulfide groups (C-S-C) and the oxidized sulfur groups (C-SO_3^-), respectively. N_{1s} peaks observed at 398.3 eV, 400.5 eV, and 4 02.5 eV were attributed to C=NH, C-NH_2, and protonated N (NH_4^+).[35,36] This observation was further evident

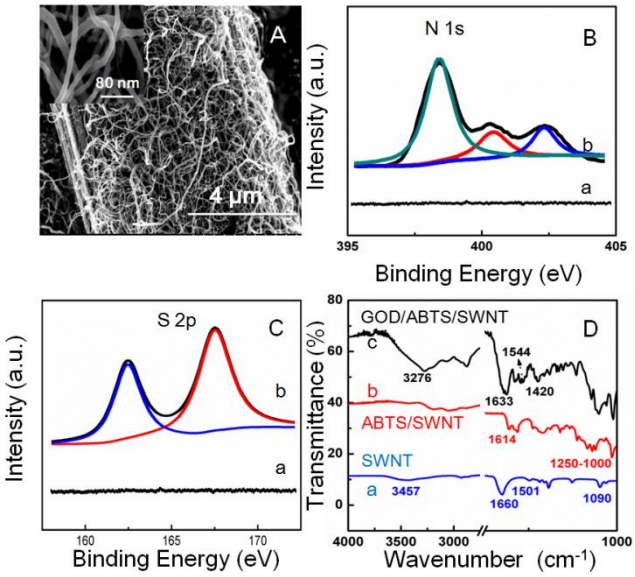

Figure 1. (A) SEM images of SWNT/CFME and the enlarged SWNT on CFME (Inset). (B and C) XPS spectra for (B) N 1s, (C) S 2p, at (a) SWNT/CFME and (b) ABTS/SWNT/CFME surfaces. (D) FTIR spectra of (a) SWNT/CFME, (b) ABTS/SWNT/CFME, and (c) GOD+ABTS/SWNT/CFME surfaces.

by FTIR spectrum shown in Figure 1D, in which the peak located at 1614 cm^{-1} corresponds to C=N stretching vibration and the peaks between 1250 cm^{-1} and1000 cm^{-1} represent S=O and S-O stretching in the -SO_3 group of ABTS.[37] All the results confirm ABTS was stably assembled onto SWNT/CFME surface. Finally, GOD molecules were immobilized onto ABTS/SWNT/CFME electrode. The modification was proved by FTIR (curve c in Figure 1D). The peak located at 1633 cm^{-1} corresponds to C=O stretching vibration of amide. The band observed at 1544 cm^{-1} was ascribed to N-H bending with a contribution from C-N stretching vibrations of amide. The peak obtained at around 3276 cm^{-1} was assigned to N-H stretching vibrations of amide. The peak located at 1420 cm^{-1} was attributed to N_5H in-plane bending vibration in FAD group. All these data indicate the successful modification of GOD on SWNT surface.[38-40] Moreover, the bioactivity of GOD molecules was maintained on ABTS/SWNT/CFME electrode.[41]

Cyclic voltammogram (CV) was then carried out to track each modification step. As demonstrated in Figure 2, only one pair of redox peak with mid-point potential ($E_{1/2}$) of 556 mV vs. Ag/AgCl was observed for ABTS/SWNT/CFME electrode in aCSF (pH 7.4), while no obvious redox peaks were obtained at CFME and SWNT/CFME electrodes. The data suggest that the observed peak at 556 mV ($E_{1/2}$) was attributed to redox peak of ABTS adsorbed on SWNT/CFME electrode. Furthermore, a pair of stable and well-defined reversible redox peak with $E_{1/2}$ of -436 mV vs. Ag/AgCl was obtained at GOD+ABTS/SWNT/CFME electrode (curve d), which was originated from direct electron transfer reaction of GOD (the conversion of FAD/$FADH_2$ center). This direct electron transfer could not be observed at GOD-modified electrode without SWNTs. The peak separation (ΔE_p) of GOD was estimated to ~33 mV at scan rate of 100 mV s^{-1} and the ratio between anodic current and cathodic one was found to be much greater than ~1.0. The observation indicates that GOD on the

ABTS/SWNT/CFME displayed a quasi-reversible electrochemical reaction despite its large molecular structure.[42] Both anodic and cathodic peak currents of GOD increased linearly with scan rates ranging from 10-400 mV s^{-1} (Figure S1). The result demonstrates that the redox reaction is a surface-confined redox process. The apparent electron-transfer rate constant (k_s) was estimated to be (6.8 ± 1.6) s^{-1}. This value was higher than those previously reported glassy carbon electrode modified with CNTs.[43]

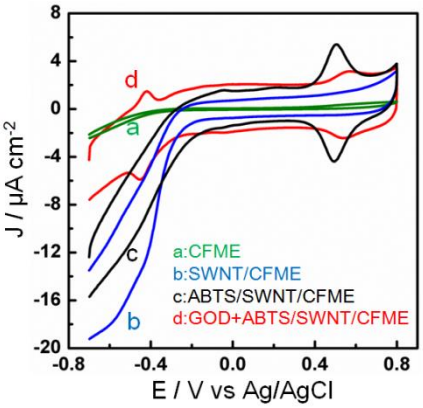

Figure 2. Cyclic voltammograms (CVs) obtained at (a) CFME, (b) SWNT/CFME, (c) ABTS/SWNT/CFME, and (d) GOD+ABTS/SWNT/CFME electrodes in aCSF solution (pH 7.4) with a scan rate of 100 mV s^{-1}.

It is well known that direct electron transfer of GOD is a two-electron along with two-proton reaction that undergoes a redox reaction as Equation (1):

$$\text{GOD (FAD)} + 2H^+ + 2e^- \leftrightarrow \text{GOD (FADH}_2\text{)} \quad (1)$$

Thus, the single redox peak of GOD can be employed for determination of both pH value (potential shift) and glucose concentration (current change). As shown in Figure 3A, the mid-point potential $E_{1/2}$ of GOD ($E_{1/2}$(GOD)) positively shifted with decreasing pH values, while $E_{1/2}$ (ABTS) located at 556 mV remained constant, resulting in ratiometric determination of pH value. The potential separation $\Delta E_{1/2}$ ($\Delta E_{1/2}$ = $E_{1/2}$(GOD)− $E_{1/2}$(ABTS) demonstrates a good linearity with varying pH from 5.67 to 7.65 with a slope of 54 mV/pH, as shown in Figure 3B. The detection limit was achieved down to 0.07 pH (3S/N). The slope was approaching the theoretical value of 58.5 mV/pH, suggesting the electrochemical process of GOD is a two-electron and two-proton reaction process.[44,45]

The electrochemical responses obtained at GOD+ABTS/SWNT/CFME electrode in aCSF solution (pH 7.4) was shown in Figure 3C. Obviously, with continuous addition of glucose, the oxidation peak current intensity (J_p) of GOD at -420 mV gradually increased, accompanied with the reduction peak current intensity decreased. As expected, the oxidation peak current intensity (J_p^0) at 567 mV ascribed to ABTS stayed almost constant. The oxidation peak current density ratio (J_p/J_p^0) obtained at -420 mV and 567 mV showed good linear relationship with the concentration of glucose in the range of 0.3-8.2 mM with the detection limit of 0.1 mM (Figure 3D). The possible mechanism could be expressed as the following equations (Equations 2 and 3):

$$\text{Glucose} + \text{GOD (FAD)} + 2e^- + 2H^+ \leftrightarrow \text{gluconolactone} + \text{GOD (FADH}_2\text{)} \quad (2)$$

$$\text{GOD (FADH}_2\text{)} + O_2 \longrightarrow \text{GOD (FAD)} + H_2O_2 \quad (3)$$

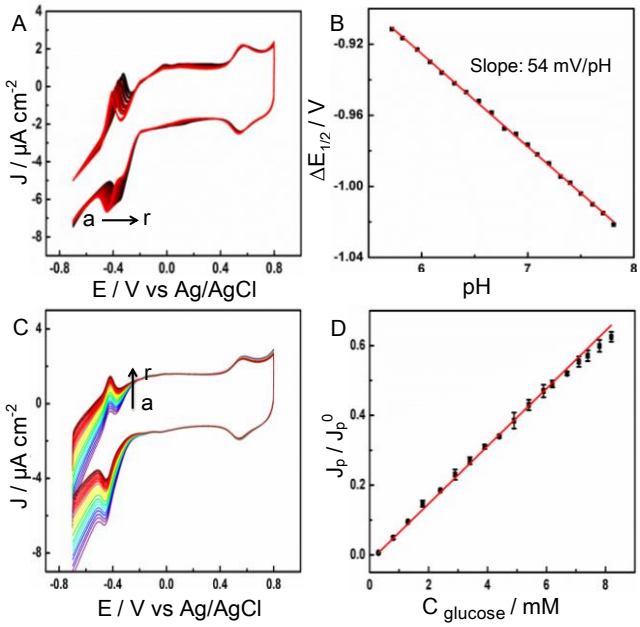

Figure 3. (A) CVs obtained at GOD+ABTS/SWNT/CFME electrode in aCSF solution with different pH values: (a-r) 7.65, 7.54, 7.43, 7.31, 7.20, 7.09, 6.97, 6.86, 6.75, 6.63, 6.52, 6.41, 6.31, 6.21, 6.10, 5.89, 5.78, and 5.67. (B) The calibration plot of $\Delta E_{1/2}$ against pH. Data were obtained from Figure 3A. (C) CVs obtained at GOD+ABTS/SWNT/CFME electrode in aCSF solution (pH 7.4) with different concentrations of glucose: (a-r) 0.3, 0.8, 1.3, 1.8, 2.4, 2.9, 3.4, 3.9, 4.4, 4.9, 5.4, 5.9, 6.2, 6.7, 7.1, 7.4, 7.8, and 8.2 mM. (D) The calibration plot of J_p/J_p^0 versus different concentrations of glucose. Data were obtained from Figure 3C.

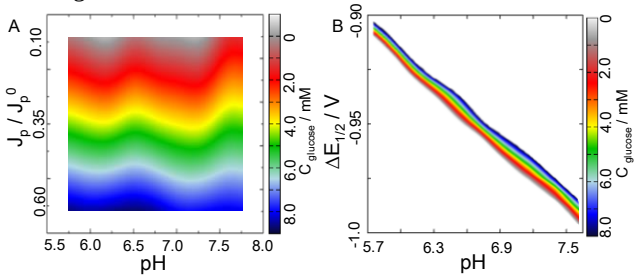

Figure 4. (A) Relational graph among J_p/J_p^0, the concentration of glucose, and pH; (B) Relational graph among $\Delta E_{1/2}$, the concentration of glucose, and pH.

More importantly, the developed GOD+ABTS/SWNT/CFME biosensor can be applied to simultaneous detection of glucose and pH. Cubic spline interpolation was used to smooth the experimental measurements. The calculation was performed using an in-house written computer program based on the functions SPLINE and SPLINT.[46] The relationship images were summarized in Figure 4, which were employed to quantify the levels of glucose and pH in the live brains.

Table 1. pH values and glucose concentrations determined by the present method in different regions of normal rat brains and rat brains of diabetic model.

	Normal rat brains				Rat brains of diabetic model			
pH	Rat 1	Rat 2	Rat 3	Mean ± SD	Rat 1	Rat 2	Rat 3	Mean ± SD
Striatum	7.3	7.2	7.3	7.3 ± 0.1	6.9	6.9	7.0	6.9 ± 0.1
Hippocampus	7.1	7.2	7.2	7.2 ± 0.1	7.1	7.0	6.9	7.0 ± 0.1
Cortex	7.3	7.2	7.3	7.3 ± 0.1	7.1	7.2	7.1	7.1 ± 0.1
Glucose (mM)								
Striatum	2.10	2.17	2.39	2.22 ± 0.18	4.21	4.56	4.82	4.53 ± 0.24
Hippocampus	1.78	1.78	1.87	1.81 ± 0.04	5.97	5.30	5.54	5.60 ± 0.27
Cortex	1.35	1.52	1.45	1.44 ± 0.12	6.45	6.56	6.94	6.65 ± 0.21

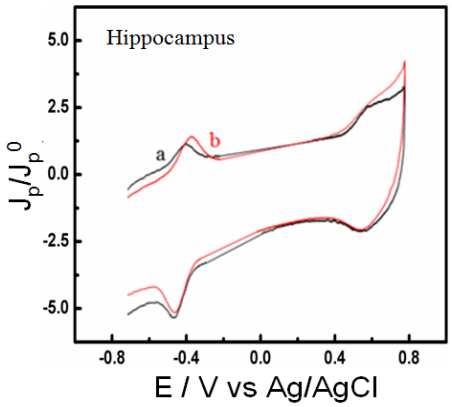

Figure 5. CVs obtained at GOD+ABTS/SWNT/CFME electrode for simultaneous determination of pH and glucose in hippocampus of (a) a normal rat brain and (b) a rat brain of diabetic model.

As mentioned above, a sensitive and accurate strategy for simultaneous determination of pH and glucose was developed. However, the complexity of brain environment may still present great challenge in selectivity of the analytical method.[47-51] The selectivity of the present GOD+ABTS/SWNT/CFME electrode was evaluated by determining the $\Delta E_{1/2}$ value and oxidation peak current density ratio (J_p/J_p^0) arising from interferences against those for pH and glucose. The potential interferences were checked, including metal ions (Na^+, K^+, Ca^{2+}, Mg^{2+}, Cu^{2+}, Zn^{2+}, Fe^{2+}, Fe^{3+}, Co^{2+}, Ni^{2+}, Cd^{2+}, Mn^{2+}), amino acids (Arg, Cys, Glu, Gly, His, Iso, Leu, Lys, Met, Phe, Ser, Thr, and Val), reactive oxygen species ($^{\cdot}OH$, $^1O_2$, $O_2^{\cdot-}$, $ROO^{\cdot}$, ClO^-, $ONOO^-$ (ROS)), and biological species (3-MT, HVA, 5-HIAA, DOPAC, ATP, DL-lactic acid, tyramine, L-tyrosine, AA, UA and DA) that may coexist in brain system. Neither shift of $\Delta E_{1/2}$ nor change of peak current density ratio (J_p/J_p^0) was observed (< 3.5%) after metal ions, amino acids, and reactive oxygen species, and biological species were added (Figure S2 A-D). For the competition test, influence of all these potential interferences on the electrochemical response to glucose was also investigated in detail. Relatively little changes (< 4.5%) were observed when all the above compounds were compared with that of glucose (Figure S2 E-H). These results demonstrated that the present GOD+ABTS/SWNT/CFME electrode possessed high selectivity for pH and glucose detection over metal ions, amino acids, typical ROS, and other biological species. In order to ensure that the developed biosensor can stably work in rat brain, the stability was also tested in aCSF (pH 7.4) via continuous cyclic voltammetric scanning for 500 cycles. The electrode showed good stability for pH and glucose determination with a negligible peak current and potential shift (Figure S3). In addition, $\Delta E_{1/2}$ and J_p/J_p^0 also stayed almost constant for six different electrodes (< 3.6%), revealing good reproducibility (Figure S4). The stability of the modified electrode in rat brain was also performed (Figure S5). No obvious changes were observed for J_p/J_p^0 (0.40%) and $\Delta E_{1/2}$ (0.21%) up to 2 h, demonstrating the long-term stability of this sensor.

The developed ratiometric biosensor with high sensitivity and selectivity based on both current and potential outputs, combined with the inherent characteristics of CFME, such as small size to minimize brain tissue damage and easy to implant, enabled us for in vivo determination of pH and glucose in a live rat brain. Figure 5 shows electrochemical responses obtained at GOD+ABTS/SWNT/CFME electrode in hippocampus of a normal rat brain (curve a) and a rat brain of diabetic model (curve b). Two pairs of peaks were obtained at GOD+ABTS/SWNT/CFME electrode in a live rat brain. It was found that $\Delta E_{1/2}$ positively shifted and oxidation peak current density ratio (J_p/J_p^0) increased in the rat brain of diabetic model, compared with those in the normal rat brain. Hence, the basal levels of pH and glucose in hippocampus of normal rat brain were estimated to be 7.2 ± 0.1 and 1.81 ± 0.16 mM, respectively (Figure 5a). Then, pH decreased to 7.0 ± 0.1 and the concentration of glucose increased to 5.60 ± 0.27 mM (Figure 5b) in hippocampus of the rat brain of diabetic model. The determined levels demonstrate similar changes with previously reported data in the rat brain of diabetic mode.[6,52,53] The levels of pH and glucose in other regions of rat brain, including striatum and cortex were also investigated and summarized in Table 1.[7,54-56] The basal levels of pH estimated to 7.3 ± 0.1 and 7.3 ± 0.1 in striatum and cortex, respectively, decreased to 6.9 ± 0.1 and 7.1 ± 0.1 in rat brains of diabetic model. On the other hand, the concentrations of glucose were found to be 2.22 ± 0.18 mM and 1.44 ± 0.12 in striatum and cortex of normal rat brains, increased to 4.53 ± 0.40 mM and 6.65 ± 0.31 mM in the rat brains of diabetic model, respectively.

CONCLUSIONS

In summary, a sensitive and selective single ratiometric biosensor for simultaneous detection and real-time quantification of pH and glucose, has been developed by using both potential and current outputs strategy. GOD has been first used as a specific recognition element for both glucose and pH. Moreover, an insensitive molecule toward pH and glucose, ABTS, has been employed as an inner-reference element to avoid the environmental effects. The present biosensor exhibits high selectivity against amino acids, metal ions, neurotransmitters, ROS, and

other biological species. Beyond this, it also demonstrates high sensitivity and accuracy in the complicated brain environment. The remarkable analytical performance of the biosensor, combined with the inherent characteristics of CFME, enables us for real-time determination the levels of pH and glucose in different region in a live rat brain of diabetic model. The detailed information on the levels of pH and glucose in normal rat brain and rat brain of diabetic model may help us to understand the damage of diabetics on brain function. The simplicity in operation and instrumentation of the biosensor should make it find broad applications in biochemical investigation. Moreover, the strategy demonstrated here could be further developed for establishing other kinds of oxidase-based biosensors with multiple outputs for in vivo applications.

ASSOCIATED CONTENT

Supporting Information

CVs obtained at GOD+ABTS/SWNT/CFME with different scan rates and relationship of peak currents versus scanning rates; selectivity and competition tests of metal ions, amino acids, neurotransmitters, ROS against glucose and pH; stability and reproducibility test. This material is available free of charge via the Internet at http:// pubs.acs.org/.

AUTHOR INFORMATION

Corresponding Author

*E-mail: ytian@chem.ecnu.edu.cn; awzhu@chem.ecnu.edu.cn; Fax: +86-21-54341041.

Notes

The authors declare no competing financial interest.

ACKNOWLEDGMENT

The authors greatly appreciate the financial support from National Natural Science Foundation of China for distinguished Young Scholars (21325521) and NSFC (21635003 and 21175098). The Program of Shanghai Subject Chief Scientist (15XD1501600) and support from China Postdoctoral Science Foundation (2014M561436 and 2016T90349) are gratefully acknowledged.

REFERENCES

(1) Schwartz, M. W.; Seeley, R. J.; Tschop, M. H.; Woods, S. C.; Morton, G. J.; Myers, M. G.; D'Alessio, D. *Nature* **2013**, *503*, 59-66.

(2) Shah, K.; DeSilva, S.; Abbruscato, T. *Int. J. Mol. Sci*. **2012**, *13*, 12629-12631.

(3) Gordijo, C. R.; Koulajian, K.; Shuhendler, A. J.; Bonifacio, L. D.; Huang, H. Y.; Chiang, S.; Ozin, G. A.; Giacca, A.; Wu, X. Y. *Adv. Funct. Mater*. **2011**, *21*, 73-82.

(4) Osundiji, M. A.; Lam, D. D.; Shaw, J.; Yueh, C. Y.; Markkula, S. P.; Hurst, P.; Colliva, C.; Roda, A.; Heisler, L. K.; Evans, M. L. *Diabetes* **2012**, *61*, 321-328.

(5) Marino, J. S.; Xu, Y.; Hill, J. W. *Trends Endocrinol. Metab.* **2011**, *22*, 275-285.

(6) Marunaka, Y.; Yoshimoto, K.; Aoi, W.; Hosogi, S.; Ikegaya, H. *Mol. Cell Therapies* **2014**, *2*, 6-8.

(7) Marunaka, Y. *World J. Diabetes* **2015**, *6*, 125-135.

(8) Wan, Q.; Chen, S.; Shi, W.; Li, L.; Ma, H. *Angew. Chem. Int. Ed*. **2014**, *53*, 10916-10920.

(9) Shi, W.; Li, X.; Ma, H. *Angew. Chem. Int. Ed.* **2012**, *51*, 6432-6435.

(10) Ding, C.; Tian, Y. *Biosens. Bioelectron*. **2015**, *65*, 183-190.

(11) Han, Y.; Ding, C.; Zhou, J.; Tian, Y. *Anal. Chem*. **2015**, *87*, 5333-5339.

(12) Huang, H.; Dong, F.; Tian, Y. *Anal. Chem*. **2016**, *88*, 12294-12302.

(13) Ma, J.; Ding, C.; Zhou, J.; Tian, Y. *Biosens. Bioelectron*. **2015**, *70*, 202-208.

(14) Zhou, J.; Zhang, L.; Tian, Y. *Anal. Chem*. **2016**, *88*, 2113-2118.

(15) Zhao, F.; Zhang, L.; Zhu, A.; Shi, G.; Tian, Y. *Chem. Commun*. **2016**, *52*, 3717-3720.

(16) Rocchitta, G.; Secchi, O.; Alvau, M. D.; Farina, D.; Bazzu, G.; Calia, G.; Migheli, R.; Desole, M. S.; O'Neill, R. D.; Serra, P. A. *Anal. Chem*. **2013**, *85*, 10282-10288.

(17) Li, R.; Guo, D.; Ye, J.; Zhang, M. *Analyst* **2015**, *140*, 3746-3752.

(18) Makos, M. A.; Omiatek, D. M.; Ewing, A. G.; Heien, M. L. *Langmuir* **2010**, *26*, 10386-10391.

(19) Jiang, Y.; Zhao, H.; Lin, Y.; Zhu, N.; Ma, Y.; Mao, L. *Angew. Chem. Int. Ed*. **2010**, *49*, 4800-4804.

(20) Zhang, L.; Han, Y.; Zhao, F.; Shi, G.; Tian, Y. *Anal. Chem*. **2015**, *87*, 2931-2936.

(21) Cao, F.; Zhang, L.; Tian, Y. *J. Electroanal. Chem*. **2016**, *781*, 278-283.

(22) Chai, X.; Zhou, X.; Zhu, A.; Zhang, L.; Qin, Y.; Shi, G.; Tian, Y. *Angew. Chem. Int. Ed.* **2013**, *52*, 8129-8133.

(23) Luo, Y.; Zhang, L.; Liu, W.; Yu, Y.; Tian, Y. *Angew.Chem. Int. Ed*. **2015,** *127*, 14259-14262.

(24) Wang, W.; Zhang, L.; Li, L.; Tian, Y. *Anal. Chem*. **2016**, *88*, 9518-9523.

(25) Lee, H.; Choi, T. K.; Lee, Y. B.; Cho, H. R.; Ghaffari, R.; Wang, L.; Choi, H. J.; Chung, T. D.; Lu, N.; Hyeon, T.; Choi, S. H.; Kim, D.-H. *Nature Nanotech.* **2016**, *11*, 566-572.

(26) Bai, H.; Han, M.; Du, Y.; Bao, J.; Dai, Z. *Chem. Commun*. **2010**, *46*, 1739-1741.

(27) Liu, G.; Paddon-Row, M. N.; Gooding, J. *J. Electrochem. Commun.* **2007**, *9*, 2218-2223.

(28) Wang, Z.; Dai, Z. *Nanoscale* **2015**, *7*, 6420-6431.

(29) Park, J. H.; Thorgaard, S. N.; Zhang, B.; Bard, A. J. *J. Am. Chem. Soc*. **2013**, *135*, 5258-5261.

(30) Zhou, J.; Booker, C.; Li, R.; Zhou, X.; Sham, T.-K.; Sun, X.; Ding, Z. *J. Am. Chem. Soc*. **2007**, *129*, 744-745.

(31) Zhang, B.; Adams, K. L.; Luber, S. J.; Eves, D. J.; Heien, M. L.; Ewing, A. G. *Anal. Chem*. **2008**, *80*, 1394-1400.

(32) Peters, J. L.; Miner, L. H.; Michael, A. C.; Sesack, S. R. *J. Neurosci. Meth.* **2004**, *137*, 9-23.

(33) Zhang, M.; Liu, K.; Xiang, L.; Lin, Y.; Su, L.; Mao, L. *Anal. Chem.* **2007**, *79*, 6559-6565.

(34) Xiang, L.; Yu, P.; Zhang, M.; Hao, J.; Wang, Y.; Zhu, L.; Dai, L.; Mao, L. *Anal. Chem*. **2014**, *86*, 5017-5023.

(35) Chen, P.; Wang, L.-K.; Wang, G.; Gao, M.-R.; Ge, J.; Yuan, W.-J.; Shen, Y. H.; Xie, A. J.; Yu, S. H. *Energy Environ. Sci*. **2014,** *7*, 4095-4103.

(36) Fu, Y.; Manthiram, A. *RSC Adv*. **2012**, *2*, 5927.

(37) Hong, J.; Xia, X.; Wang, Y.; Xu, R. *J. Mater. Chem. B* **2012**, *22*, 15006-15009.

(38) Portaccio, M.; Della Ventura, B.; Mita, D. G.; Manolova, N.; Stoilova, O.; Rashkov, I.; Lepore, M. *J. Sol-Gel Sci. Tech.* **2011**, *57*, 204-211.

(39) Salimi, A.; Noorbakhsh, A. *Electrochim. Acta* **2011**, *56*, 6097-6105.

(40) Fang, B.; Zhang, C.; Wang, G.; Wang, M.; Ji, Y. *Sens. Actuators, B: Chem* **2011**, *155*, 304-310.

(41) Zuo, S.; Teng, Y.; Yuan, H.; Lan, M. *Sens. Actuators, B: Chem* **2008**, *133*, 555-560.

(42) Liu, Y.; Wang, M.; Zhao, F.; Xu, Z.; Dong, S. *Biosens. Bioelectron.* **2005**, *21*, 984-988.

(43) Liu, J.; Chou, A.; Rahmat, W.; Paddon-Row, M. N.; Gooding, J. *J. Electroanalysis* **2005**, *17*, 38-46.

(44) Cheer, J. F.; Wassum, K. M.; Wightman, R. M. *J. Neurochem.* **2006**, *97*, 1145-1154.
(45) Lu, M.; Compton, R. G. *Analyst* **2014**, *139*, 2397-2403.
(46) Press, W. H.; Teukolsky, S. A.; Vetterling, W. T.; Flannery, B. P. Numerical Recipes in C. Cambridge University Press, Cambridge, 1992.
(47) Chen, Z.; Hayashi, K.; Iwasaki, Y.; Kurita, R.; Niwa, O.; Sunaawa, K. *Electroanalysis* **2005**, *17*, 231-238.
(48) Niwa, O.; Horiuchi, T.; Kurita, R.; Torimitsu, K. *Anal. Chem.* **1998**, *70*, 1126-1132.
(49) Keighron, J. D.; Akesson, S.; Cans, A. S. *Langmuir* **2014**, *30*, 11348-11355.
(50) Keighron, J. D.; Wigstrom, J.; Kurczy, M. E.; Bergman, J.; Wang, Y.; Cans, A. S. *ACS Chem. Neurosci.* **2015**, 6, 181-188.
(51) Kulagina, N. V.; Shankar, L.; Michael, A. C. *Anal. Chem.* **1999**, *71*, 5093-5100.
(52) Kealy, J.; Bennett, R.; Lowry, J. P. *J. Neurosci. Methods* **2013**, *215*, 110-120.
(53) Alipour, M.; Salehi, I.; Ghadiri Soufi, F. *Stroke* **1991**, *22*, 505-509
(54) Herzog, R. I.; Chan, O.; Yu, S.; Dziura, J.; McNay, E. C.; Sherwin, R. S. *Endocrinology* **2008**, *149*, 1499-1504.
(55) Lind, K. R.; Ball, K. K.; Cruz, N. F.; Dienel, G. A. *Neurochem. Int.* **2013**, *62*, 784-795.
(56) Netchiporouk, L. I.; Shram, N. F.; Jaffrezic-Renault, N.; Martelet, C.; Cespuglio, R. *Anal. Chem.* **1996**, *68*, 4358-4364.

Table of Contents